



Effects of high-voltage power sources on fine particle collection efficiency with an industrial electrostatic precipitator

Jibao Zhu^a, Qinxia Zhao^b, Yuping Yao^b, Shikai Luo^b, Xiaochuan Guo^b, Xuming Zhang^a, Yuxuan Zeng^a, Keping Yan^{a,*}

^aKey Laboratory of Biomass Chemical Engineering of Ministry of Education, Zhejiang University, Hangzhou 310027, China

^bFeida Environmental Science and Technology Co. Ltd, Zhuji 311800, China

ARTICLE INFO

Article history:

Received 31 August 2011
Received in revised form
4 February 2012
Accepted 21 March 2012
Available online 7 April 2012

Keywords:

Electrostatic precipitation
Corona
PM2.5
Particles
High-voltage power source

ABSTRACT

This paper presents industrial investigations on fine particle grade collection efficiency of an industrial electrostatic precipitator (ESP). Experiments are performed with a hybrid ESP and fabric filter (FF). Gas flow rates, mass inlet concentration, gaseous temperature and the ESP plate–plate distance are 20,000–40,000 Nm³/h, 15 g/Nm³, 110 °C, and 400 mm, respectively. The ESP specific collection area ranges from 10 to 20 m²/m³/s. Both single-phase and three-phase transformer-rectifiers (TRs) are used for energizing the ESP. When changing the single-phase TR to the three-phase TR, the maximum average secondary voltage is increased from 55 kV to 71 kV and average corona current rises from 31 mA to 62 mA without spark breakdown. As a result, both fine particle grade collection efficiency $\eta(r)$ and their migration velocities are significantly increased. With the single-phase TR, the velocity is around 17 cm/s for all particles. With three-phase TR, its maximum value is about 35 cm/s. For particles within 0.03–0.1 μm and 0.1–2.5 μm in diameter, the efficiencies rise from about 85% to 95% and 92, respectively. For particles of around 2.5–8.0 μm , they rise from about 87% to about 98%. Moreover, experiments show that a revised Deutsch equation $\log(1 - \eta(r))/\beta = -\alpha E_a^2 S$ gives a good approximation via the average electric field E_a , the specific collection area S and two correction coefficients α and β , which depend on particle size.

© 2012 Elsevier B.V. All rights reserved.

1. Introduction

Over the past century, electrostatic precipitators (ESPs) have been widely used in industries for particle collection due to their high efficiency and low cost [1,2]. Its state of art of fundamentals and mechanical design, models, electrical operation and power sources, conditioning, hybrid precipitation techniques, and industrial applications can be referred to the latest ESP proceedings [3]. Today, world-wide evaluation on health impact of fine particles have promoted a number of campaigns for understanding particulate matter (PM) emission from combustion sources and their concentration in air. For examples, Ehrlich et al. reported PM emission from 303 plants and domestic stoves in Germany [4]. Zhao et al. estimated Chinese PM emission after evaluation of ten Chinese coal-fired power plants [5]. Khan and Sun et al. presented PM characteristics around Yokohama and Beijing, respectively [6,7]. On the other hands, world-wide ESP upgrading has obtained

significant achievements for reducing PM emission and/or saving energy consumption. With regard to Chinese utilities [5,8], almost all ESPs need to be upgraded by considering PM2.5 emission (particles with a diameter of less than 2.5 μm). Industrial observations have indicated that a poor ESP performance is always related to either back corona or insufficient particle charging at the inlet field of the ESP or both of them. Retrofitting usually includes resizing ESP itself, changing it to hybrid ESP & FF (Fabric Filter) precipitator [9], replacing high-voltage (HV) and/or low-voltage (LV) power sources [10,11], coal switching, flue gas conditioning or using pre-charger [12]. A number of literature are available for those individual applications [3]. Among them, one of the most cost effective techniques is to upgrade the HV power sources by using the latest automatic voltage controller (AVC) and/or new types of HV techniques, such as by using switch-mode power supplies [3]. For 400 mm gap ESPs, typical used output voltage and current of three-phase TRs are 82 kV and 2.0 A, respectively, which are beyond switch-mode power sources. Our industrial applications to 125 MW, 300 MW and 600 MW Chinese coal-fired boilers have confirmed that after retrofitting traditional single-phase TRs at the inlet ESP field, both the corona discharge power and the particle

* Corresponding author. Fax: +86 571 88210340.
E-mail address: kyan@zju.edu.cn (K. Yan).

collection efficiency significantly rise. The specific collection area of the inlet field is usually around $10\text{--}20\text{ m}^2/\text{m}^3/\text{s}$ [13]. Detailed principles for upgrading ESP to reduce emission and save energy consumption, however, are not available yet due to our poor knowledge on PM_{2.5} emission in terms of specifications of ESP collection area, particle characteristics and the high-voltage power sources.

This paper reports our continuous work on ESP upgrading by using the three-phase TR and fine particle grade collection efficiency. Its main objective is to get deep insights on the fine particle migration velocities and to provide simplifying collection approximations in terms of the applied electric field, the specific collection area and particle size for upgrading industrial ESPs.

2. Pilot experimental setup

The pilot hybrid precipitator as shown in Fig. 1 consists of two parts, namely the first-stage ESP and the second-stage FF. The precipitator is installed in-parallel to a full-scale FF in order to adjust the gas flow rate from $20,000\text{ Nm}^3/\text{h}$ to $40,000\text{ Nm}^3/\text{h}$. Flue gas firstly enter the ESP and then the FF. The hybrid precipitator was carefully designed by considering gas flow distribution and system pressure drop. The same type of precipitator has been used for up to 600 MW coal-fired generator. The system has been in operation for over two years with a local 30 MW coal-fired power generator. The gap between ESP plates is 400 mm. The length and height of ESP are 2500 mm and 4200 mm, respectively. The ribbed strike type electrode is used for the corona wire. The maximum gas velocity at $110\text{ }^\circ\text{C}$ inside the ESP is 1.15 m/s under $40,000\text{ Nm}^3/\text{h}$. The specifications of the experimental setup are listed in Table 1.

An in-situ electrical low-pressure impactor (ELPI) is used to analyze particle concentration and size distribution. The ELPI is a 13-stage low-pressure cascade impactor. The size range is from 30 nm to $10\text{ }\mu\text{m}$. The technique has been widely used for studying PM emission [5]. Its detailed diagnostic principle was early reported [14]. Particle sampling ports are located at the ESP and FF outlets, respectively. All experimental data are obtained between two rapping cycles. The initial inlet particle specifications are obtained by means of the measurement at the ESP outlet when switching off the power source. Particle natural collection inside the ESP is excluded for evaluation of the collection efficiency. Particle concentrations are obtained by averaging individual

Table 1
List of the specifications of the precipitator.

Unit	Value
Flow gas	
Gas flow rate (m^3/h)	40,000
Inlet gas temp ($^\circ\text{C}$)	110 (max.120)
Inlet dust (g/Nm^3)	15
ESP	
Total cross area (m^2)	9.6
Total ESP length (mm)	2500
Total ESP height (mm)	4200
Plate–plate distance (mm)	400
Total collector surface (m^2)	120
Total length of corona wire (m)	120
Gas velocity inside ESP (m/s)	1.15
Specific collecting area (SCA)	10.9
FF	
Fabric filter	PPS
Total cloth area (m^2)	333
Filter velocity	2 m/min

sampled data across these outlet sections. Within this study, the total inlet mass concentration is around $15\text{ g}/\text{Nm}^3$ with an average diameter of $11.2\text{ }\mu\text{m}$ and a specific dust resistivity of $3.09 \times 10^{10}\text{ }\Omega\text{ cm}$ at $110\text{ }^\circ\text{C}$. Detailed evaluation of dust resistivity was reported in Ref. [15].

Both single-phase and three-phase TRs were used in order to carry out a series of comparison experiments. For each observation, experiments were usually performed within a week. And then the collected data were analyzed according to operation conditions. Fig. 2 shows circuit diagrams of the traditional single-phase and three-phase TRs. Both primary and secondary voltage and current were automatically measured with an equipped AVC [16]. The single-phase TR is based on a couple of anti-parallel silicon controlled rectifiers. Its operation principle and various control methodologies have been very well described [2]. The three-phase TR is based on three couples of anti-parallel silicon controlled rectifiers. The technique has been known for many years. Few reports, however, are available for discussing its performances on particle grade collection efficiency. As far as we know, the work by Boyle and Paradiso is the only available literature to discuss the issue by means of an opacity monitor. The comparison experiments of three-phase TR with single-phase TR were also performed under the same industrial conditions [17].

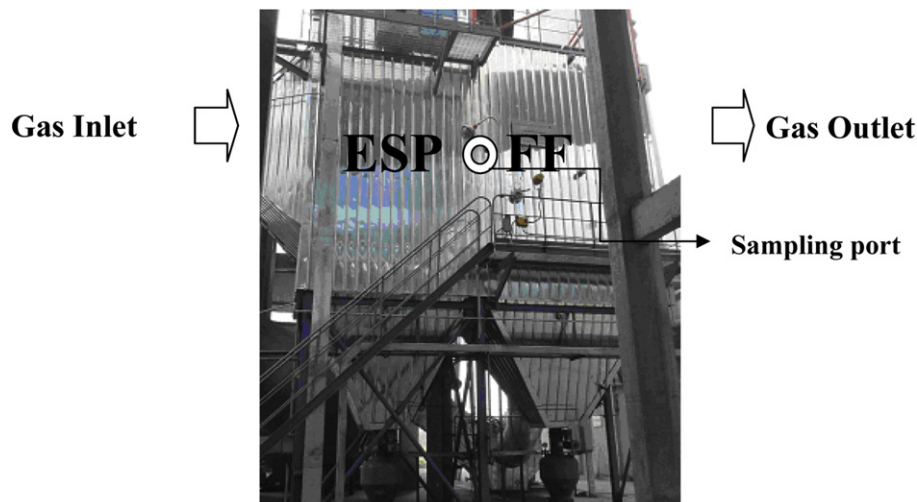


Fig. 1. Photo of the pilot experimental setup.

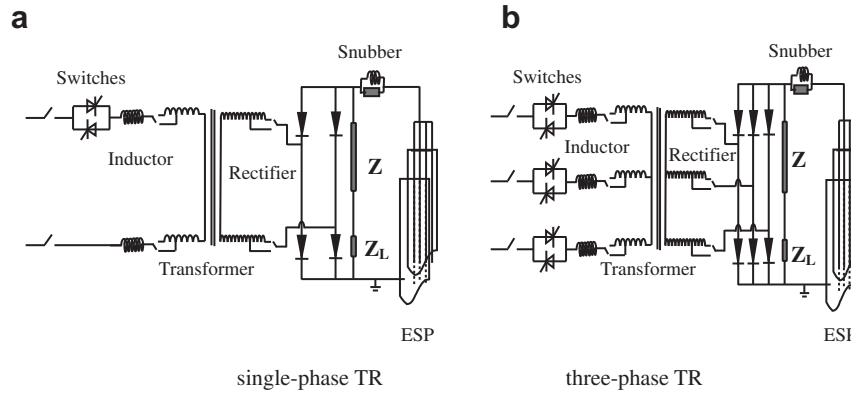


Fig. 2. Circuit diagrams of single-phase and three-phase TRs, where Z and Z_L refer to the resistors used for a voltage divider.

3. Experimental results and discussions

3.1. Secondary voltage and current I–V characteristics

Time-resolved voltage and current waveforms and average secondary voltage V_a and current characteristics are used to study the I–V curves. Fig. 3 shows typical waveforms of the secondary voltage and current. Referring to the current waveform with the single-phase TR, it always drops to zero when the voltage rises to its maximums. For three-phase TR, however, it almost keeps a constant value without drops to zero at all, which in fact require a new type of AVC for controlling spark breakdowns [13]. With regard to the voltage waveforms, the voltage ripple significantly becomes smaller when using the three-phase TR. Its V_a and its peak voltage V_p are almost identical. As a result, the I–V curves shows very distinguished features as illustrated in Fig. 4. For the single-phase TR, the ratio of $(V_p - V_a)/V_a$ is around 30–40%. For three-phase TR, however, it is less than 5%. Within present work, by changing the single-phase TR to the three-phase TR, the maximum applied secondary voltage V_a and current rise from 55 kV to 71 kV and from 31 mA to 62 mA, respectively. The corona power is increased by a factor of 2.5. Moreover, the observed voltage and current curves are in agreements with the early reported phenomena [13,17]. Namely, for a given secondary voltage, the average current is always

smaller when using three-phase TR; and for a given current, the secondary voltage always becomes higher as shown in Fig. 4. For a given ESP, the maximum $V_a V_p$ value can be greatly increased with three-phase TR because V_a is almost equal to V_p . According to those arguments, the ESP collection efficiency is anticipated to be improved when retrofitting single-phase TR to three-phase TR.

3.2. Grade collection efficiencies in terms of particle number concentration

In order to present the effects of three-phase TR on ESP’s performance, we use the following nomenclatures:

- r Aerodynamic radius of particle r , (μm)
- $\eta(r)$ Grade collection efficiency in terms of particle numbers with a radius of r , (%)
- $N_i(r)$ Particle number concentration at the ESP inlet with a radius of r , ($1/\text{cm}^3$)
- $N_o(r)$ Particle number concentration at the ESP outlet with a radius of r , ($1/\text{cm}^3$)
- $\omega(r)$ Migration velocity of particles with a radius of r , (cm/s)
- η_{r1-r2} Grade mass collection efficiency of particles with a radius from r_1 to r_2 , (%)
- E_a Average electric field inside the ESP in terms of the average voltage V_a , (kV/cm)

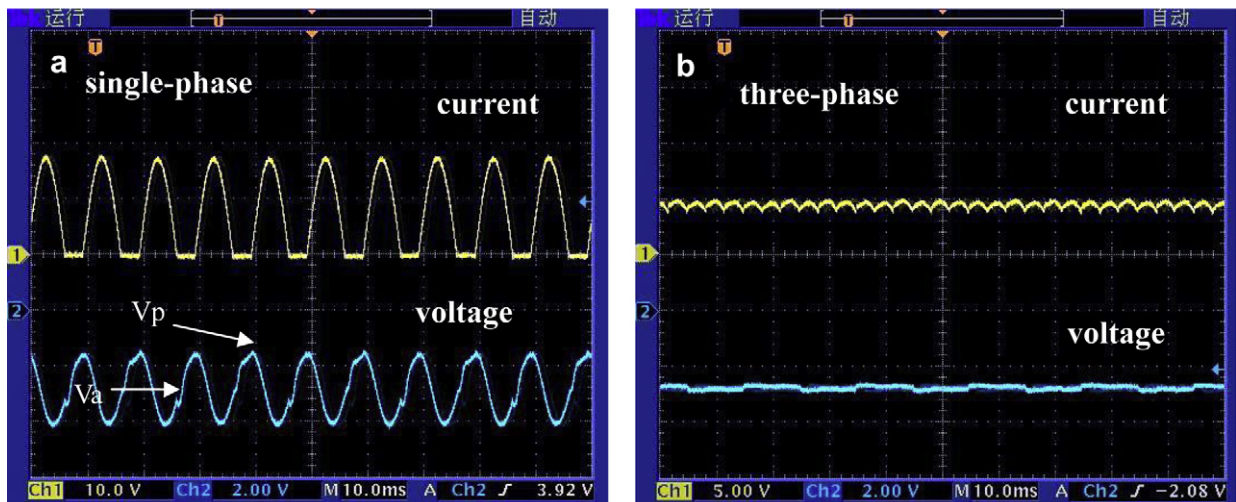


Fig. 3. Time-resolved characteristics of secondary voltage and current waveforms via 20 ms/div, a) with single-phase TR, b) with three-phase TR.

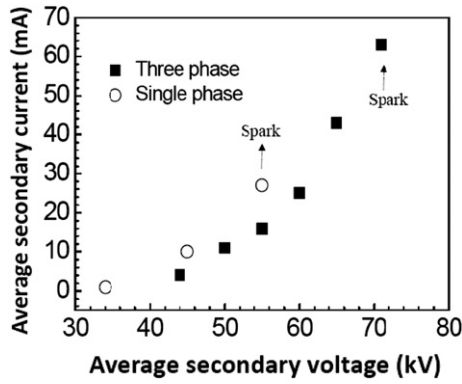


Fig. 4. Averaged secondary voltage and current I–V curves under a gas low rate of 40,000 Nm³/h and an initial mass concentration of 15 g/Nm³ at 110 °C.

E_p Average electric field inside the ESP in terms of the peak voltage V_p , (kV/cm)

S Specific collection area of the ESP, (m²/m³/s)

Thus, by definitions and according to the original Deutsch approximation [2], we have following equations:

$$\eta(r) = 1 - \frac{N_o(r)}{N_i(r)} \quad (1)$$

$$\eta_{r_1-r_2} = 1 - \frac{\sum_{r_1}^{r_2} [1 - \eta(r)] \cdot N_i(r) \cdot r^3}{\sum_{r_1}^{r_2} N_i(r) \cdot r^3} \quad (2)$$

$$\eta(r) = 1 - \exp[-\omega(r) \cdot S] \quad (3)$$

where, all particles are supposed to have the same mass density.

Fig. 5 shows typical ESP inlet $N_i(r)$ and outlet $N_o(r)$ number distributions when the three-phase TR is operated at 69 kV and 62 mA. Fig. 6 compares the effects of the power sources on the grade collection efficiencies. For both single and three-phase TRs, the efficiency $\eta(r)$ always rises with increasing the applied voltage. With the single-phase TR at its maximum operation voltage of 55 kV, it is around 83–88%. With three-phase TR at 69 kV, it rises to about 92–98%. With refer to the original Deutsch approximation (3), the derived migration velocity are plotted in Fig. 7. For the single-phase TR, it is not significantly dependent on the particle diameters. It is around 17 cm/s in average. For three-phase TR, however, the migration velocities for both ultra-fine particles (<0.1 μm) and particles (>2.5 μm) significantly depend on the diameter with a maximum of about 35 cm/s. For fine particles

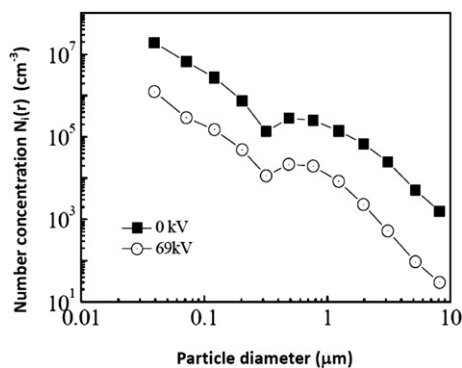


Fig. 5. ESP inlet and outlet particle size distributions under a gas low rate of 40,000 Nm³/h and an initial mass concentration of 15 g/Nm³ at 110 °C.

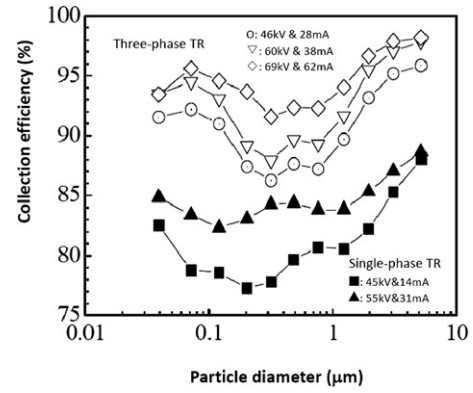


Fig. 6. Grade collection efficiency versus particle diameter and power sources under a gas low rate of 40,000 m³/h and an initial mass concentration of 15 g/Nm³ at 110 °C.

(0.1–2.5 μm), it is about 25 cm/s. With regard to the approximation relation between the migration velocity, the particle radius and the electric fields as theoretically discussed in literature [18], experiments hardly show any simplifying correlation. The original Deutsch equation needs to be revised as far as the particle grade collection efficiency is considered. Electro-hydrodynamic flow and back corona significantly affect the relationship [19,20]. As far as the effects of the applied electric field square $E_a E_p$ and the specific collection area is concerned, details are discussed in terms of the ESP performance curves.

3.3. Grade collection efficiencies in terms of particle mass concentration

It is very well known that the Deutsch equation is based on two simplifying assumptions: 1) all particles are fully charged and uniformly distributed in any ESP cross section, 2) the migration velocity is identical for all particle size for calculating the total mass collection. Referring to Fig. 7, one can easily conclude that it is almost impossible to give an identical migration velocity for industrial ESP design when considering the grade collection efficiency. This argument can be further confirmed in terms of the particle penetration $1 - \eta(r)$ and the specific collection area S as shown in Figs. 8 and 9, where experiments were performed at a given applied voltage but with three gas flow rates of 20,000, 30,000 and 40,000 Nm³/h correspond to the S values of 21.6, 14.4, 10.9 m²/m³/s, respectively. According to those experimental

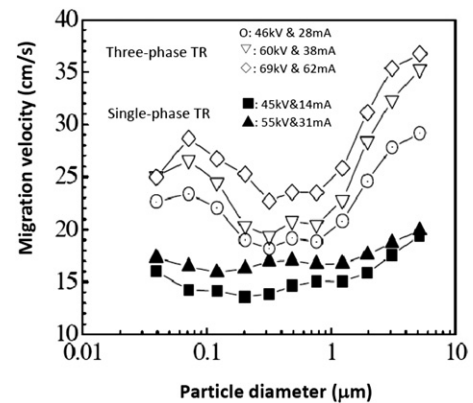


Fig. 7. Migration velocity versus particle diameter and power sources under a gas low rate of 40,000 m³/h and an initial mass concentration of 15 g/Nm³ at 110 °C.

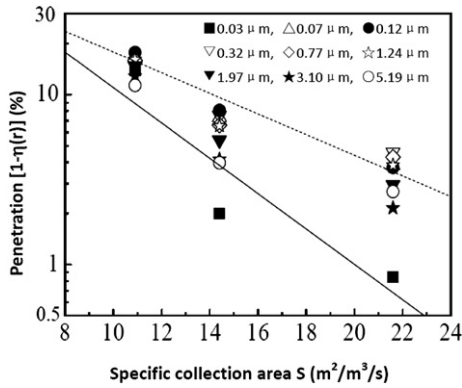


Fig. 8. Grade penetration versus the specific collection area and particle diameters with the single-phase TR at its averaged voltage and current of 55 kV and 31 mA. The inlet mass concentration and temperature are 15 g/Nm³ and 110 °C, respectively.

observations, we propose a revised grade collection or penetration approximation as:

$$\log \frac{1 - \eta(r)}{\beta} = -\alpha \cdot E_a \cdot E_p \cdot S \quad (4)$$

$$\omega(r) = \alpha \cdot E_a \cdot E_p \quad (5)$$

where, α and β are defined correction coefficients.

The linear relationship between the penetration $\log [1 - \eta(r)]$ and the specific collection area S exist for single and three-phase TRs as shown in Figs. 8 and 9. The correction coefficients, however, significantly depends on the particle diameters and the specifications of the sources. Within the present work, the minimum penetration with single-phase TR is around 5–15% at 55 kV. With three-phase TR, however, it drops to about 2–5% at 69 kV. The equation (4) has a similar form as the extended Deutsch equation when considering the mechanical collection efficiency [21], the equation proposed here, however, have excluded the mechanical effects as the particle initial inlet concentrations are measured at the ESP outlet when switching off its power source.

With regard to mass grade collection efficiency η_{r1-r2} or its penetration as described by equation (4), we divide the particles into three groups, namely ultra-fine (0.03–0.1 μm), fine (0.1–2.5 μm) and particles (2.5–8.0 μm). Their grade mass penetration curves via the specific collection area (S) are plotted in Figs. 10 and 11 for single and three-phase TRs, respectively. The

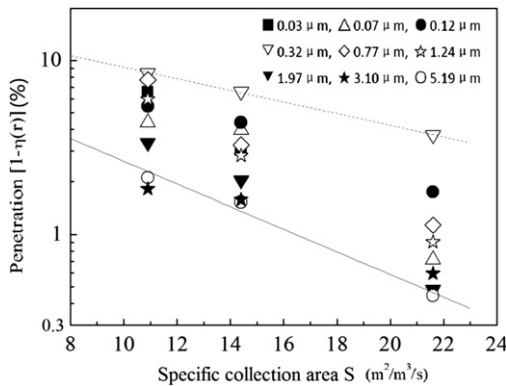


Fig. 9. Grade penetration versus the specific collection area and particle diameters with the three-phase TR at its averaged voltage and current of 69 kV and 62 mA. The inlet mass concentration and temperature are 15 g/Nm³ and 110 °C, respectively.

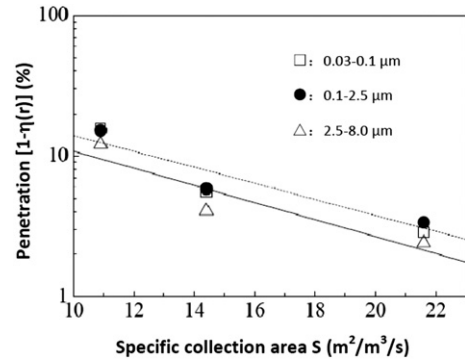


Fig. 10. Grade mass penetration versus the specific collection area and the particle sizes with the single-phase TR at 55 kV and 32 mA. The initial mass concentration and temperature are 15 g/Nm³ and 110 °C, respectively.

modified Deutsch equation (4) can give very good estimation for all particles. For ultra-fine and fine particles, their migration velocities are almost identical. For particles (2.5–8.0 μm), however, their migration velocity rises by factors of 1.12 and 1.18 for single and three-phase TRs, respectively.

As far as the dependence of the grade collection efficiency on the average electric field (E_a) with three-phase TR, Figs. 12 and 13 show particle number and mass penetration, respectively, where the same values of the peak and average voltages are used. For a given S value, the modified Deutsch approximation gives very good estimation for their mass collection in terms of the square of the average electric field. And for ultra-fine and fine particles, their migration velocities are almost identical. For particles (2.5–8 μm), their mass migration velocity rises by a factor of 1.31. According to these results, one can easily conclude that when resizing ESP for further reducing particle emission, the migration velocity used for designing the ESP can no longer be used for resizing. It must be corrected according the grade efficiencies as illustrated in Fig. 13.

3.4. Particle grade collection efficiency with multi-electric fields

Industrial ESPs usually consist of several electric fields. Today, it is very common to have 4 or 5 electric fields with a total specific collection area of around 100–120 m²/m³/s. Supposing an ESP with n electric fields, then, we have the following relation for its i th field:

$$\log \frac{1 - \eta_i(r)}{\beta_i} = -\alpha_i E_{ai}^2 S_i \quad \text{for } 1 \leq i \leq n \quad (6)$$

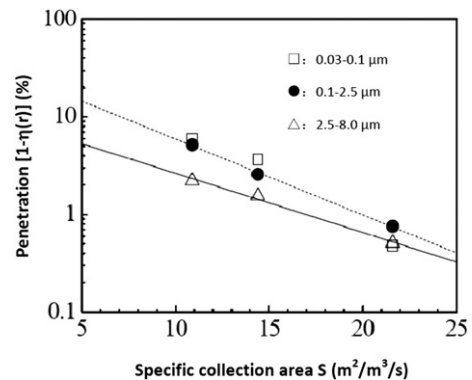


Fig. 11. Grade mass penetration versus the specific collection area and the particle sizes with the three-phase TR at 69 kV and 62 mA. The initial mass concentration and temperature are 15 g/Nm³ and 110 °C, respectively.

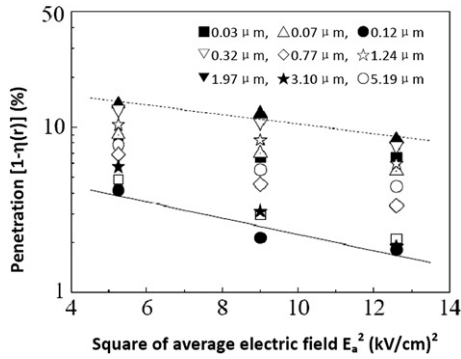


Fig. 12. Grade particle penetration versus the applied electric field and particle diameter with the three-phase TR under the flow rate of 40,000 m³/h and gas temperature of 110 °C, and initial concentration of 15 g/Nm³.

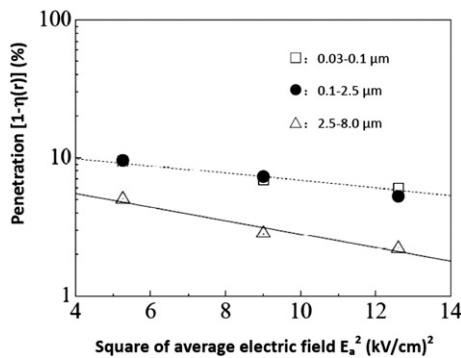


Fig. 13. Grade mass penetration versus the applied electric field and particle sizes with the three-phase TR under the flow rate of 40,000 m³/h and gas temperature of 110 °C, and initial concentration of 15 g/Nm³.

where $\eta_i(r)$, E_{ai} , S_i , α_i and β_i have the same meaning as described above except they refers to the i th field. Thus, the total penetration can be derived as:

$$1 - \eta(r) = \prod_1^n (1 - \eta_i(r)) \quad (7)$$

Substituting equation (6) into the above equation, we get:

$$\log \frac{1 - \eta(r)}{\prod_1^n \beta_i} = - \sum_1^n \alpha_i E_{ai}^2 S_i \quad (8)$$

Industrial ESPs are often designed with identical specific collection area S_i for each field, thus, the equation (8) can be further simplified as the following equation (9) by defining the average electric field and the correction coefficients α and β as: $\alpha E_a^2 = \sum_1^n \alpha_i E_{ai}^2 / n$ and $\beta = \prod_1^n \beta_i$, respectively.

$$\log \frac{1 - \eta(r)}{\beta} = -\alpha E_a^2 S \quad (9)$$

where S is the total collection area as $S = nS_i$.

4. Conclusions

According to a series of industrial demonstration experiments with both single-phase and three-phase TRs, we can give the following concluding remarks:

- 1) In terms of either the specific collection area or the applied electric fields, both the particle number and mass grade collection efficiencies can be very well estimated with a modified Deutsch equation provided that the coefficients are corrected according to both the applied electric field and the particle diameters. There is no simplifying equation, however, to give analytic relation between the migration velocity and the particle diameters yet.
- 2) In contrast to using single-phase TR, with three-phase TRs, particle grade collection efficiencies of the inlet field of ESP can be significantly improved due to its higher applied voltage and larger corona current. For ultra-fine particle of 0.03–0.1 μm, it is improved by a factor of about 1.12. For fine particles of 0.1–2.5 μm, it is by about 1.08, and for particles of 2.5–8 μm, it becomes about 1.13.
- 3) When resizing ESP to further reduce mass emission concentration, the migration velocity used for designing the old ESP cannot be used for simplifying the new part of the ESP as it is significantly dependent on the particle size. For the inlet field of the ESP, the mass collection efficiency can be increased from about 80–85% to 90–95% when upgrading traditional single-phase TRs by using three-phase TRs. According to the modified Deutsch equation, it becomes possible to predicate ESP performance after upgrading the power source and/or resizing the ESP itself. It is expected that a number of Chinese ESP for electricity and steel industries can be upgraded with the three-phase TR in the near future. Detailed coefficients, however, need to be evaluated according to individual applications.

Acknowledgments

This study is supported by the Chinese 863 fund via the project 2007AA061804, Hangzhou Sci. & Tech. fund via the project 20080213A15, Chinese NSFC via the project N10711, and the R&D fund of Zhejiang Provincial Engineering Research Center of Industrial Boiler & Furnace Flue Gas Pollution Control.

References

- [1] Series publications of Electrostatic Precipitation, <http://www.isesp.org/>.
- [2] S. Oglesby, G.B. Nichols, Electrostatic Precipitation, Marcel Dekker Inc., New York, 1978.
- [3] Electrostatic precipitation, in: K. Yan (Ed.), 11th International Conference on Electrostatic Precipitation, Springer-Verlag GmbH, Berlin Heidelberg, Hangzhou, 2008.
- [4] C. Ehrlich, G. Noll, W.D. Kalkoff, G. Baumbach, A. Dreiseidler, PM 10, PM 2.5 and PM 1.0-emissions from industrial plants-results from measurement programmes in Germany, Atmos. Environ. 4 (2007) 6236–6254.
- [5] Y. Zhao, S. Wang, C.P. Nielsen, X. Li, J. Hao, Establishment of a database of emission factors for atmospheric pollutants from Chinese coal-fired power plants, Atmos. Environ. 44 (2010) 1515–1523.
- [6] M.F. Khan, Y. Shirasuna, K. Hirano, S. Masunaga, Characterization of PM_{2.5}, PM_{2.5-10} and PM_{>10} in ambient air, Yokohama, Japan, Atmos. Res. 96 (2010) 159–172.
- [7] J. Sun, Q. Zhang, M.R. Canagaratna, Y. Zhang, N.L. Ng, Y. Sun, J.T. Jayne, X. Zhang, X. Zhang, D.R. Worsnop, Highly time- and size-resolved characterization of submicron aerosol particles in Beijing using an Aerodyne Aerosol Mass Spectrometer, Atmos. Environ. 44 (2010) 131–140.
- [8] Q. Yao, S.Q. Li, H.W. Xu, J.K. Zhuo, Q. Song, Studies on formation and control of combustion particulate matter in China: a review, Energy 34 (2009) 1296–1309.
- [9] F.J. Gutiérrez Ortiz, B. Navarrete, L. Cañadas, L. Salvadora, A technical assessment of a particle hybrid collector in a pilot plant, Chem. Eng. J. 127 (2007) 131–142.
- [10] K. Parker, A.T. Haaland, F. Vik, Enhanced fine particle collection by the application of SMPS energisation, J. Electrostat. 67 (2009) 110–116.
- [11] N. Grass, W. Hartmann, M. Klockner, Application of different types of high-voltage supplies on industrial electrostatic precipitators, IEEE Trans. Ind. Appl. 6 (2004) 1513–1520.
- [12] J. Zhu, X. Zhang, W. Chen, Y. Shi, K. Yan, Electrostatic precipitation of fine particles with a bipolar pre-charger, J. Electrostat. 68 (2010) 174–178.

- [13] B. Zhang, R. Wang, K. Yan, Industrial applications of three-phase TR for upgrading ESP performance, in: K. Yan (Ed.), *Electrostatic Precipitation ICESPXI*, Springer-Verlag GmbH, Berlin Heidelberg, Hangzhou, 2008, pp. 276–280.
- [14] J. Ristimäki, A. Virtanen, M. Marjamäki, A. Rostedt, J. Keskinen, On-line measurement of size distribution and effective density of submicron particles, *J. Aerosol Sci.* 33 (2002) 1541–1557.
- [15] X. Li, X. Zhang, J. Zhu, W. Feng, K. Yan, Sensitivity analysis on the maximum ash resistivity in terms of its compositions and gaseous water concentration, *J. Electrostat.* 70 (2012) 83–90.
- [16] J. Ma, Y. Yang, R. Wang, K. Yan, Industrial applications of a new AVC for upgrading ESP to save energy and improve efficiency, in: K. Yan (Ed.), *Electrostatic Precipitation ICESPXI*, Springer-Verlag GmbH, Berlin Heidelberg, Hangzhou, 2008, pp. 281–283.
- [17] P.D. Boyle, G. Paradiso, Demonstration of Three Phase Power Supply for Electrostatic Precipitators, , In: *Proceedings of the American Power Conference*, vol. 61-1, Illinois Institute of Technology, Chicago, IL, 1999.
- [18] S. Masuda, S. Hosokawa, Electrostatic precipitation, in: J.S. Chang, A.J. Kelly, J.M. Crowley (Eds.), *Handbook of Electrostatic Processes*, Marcel Dekker, Inc., New York, 1995, pp. 441–479.
- [19] J. Podliński, A. Niewulis, J. Mizeraczyk, Electrohydrodynamic flow and particle collection efficiency of a spike-plate type electrostatic precipitator, *J. Electrostat.* 67 (2009) 99–104.
- [20] T. Iváncsy, I. Kiss, I. Berta, Improved model for the analysis of back corona in pulse energised electrostatic precipitators, *J. Electrostat.* 67 (2009) 146–149.
- [21] C. Paulson, Precipitator sizing methods, in: K.R. Parker (Ed.), *Applied Electrostatic Precipitation*, Blackie Academic & Professional, London, 1997, pp. 252–279.